



## Molecular Crystals and Liquid Crystals Science and Technology. Section A. Molecular Crystals and Liquid Crystals

Publication details, including instructions for authors and subscription information:

<http://www.tandfonline.com/loi/gmcl19>

## Static and Dynamic Observations of Dislocations and Other Defects in Smectic Cano Wedges

I. Lelidis<sup>a b</sup>, M. Kléman<sup>c</sup> & J. L. Martin<sup>a</sup>

<sup>a</sup> Département de Physique, Institut de Genie Atomique, Ecole Polytechnique Fédérale de Lausanne, CH-1015, Lausanne, Switzerland

<sup>b</sup> LPMC Université de Picardie, 80039, Amiens, France

<sup>c</sup> Laboratoire de Minéralogie-Cristallographie (CNRS-UMR 7590, Universités de Paris VI et Paris VII), 4 place Jussieu, 75252, Paris, Cedex, 05, France

Version of record first published: 24 Sep 2006

To cite this article: I. Lelidis, M. Kléman & J. L. Martin (2000): Static and Dynamic Observations of Dislocations and Other Defects in Smectic Cano Wedges, Molecular Crystals and Liquid Crystals Science and Technology. Section A. Molecular Crystals and Liquid Crystals, 351:1, 187-196

To link to this article: <http://dx.doi.org/10.1080/10587250008023268>

Full terms and conditions of use: <http://www.tandfonline.com/page/terms-and-conditions>

This article may be used for research, teaching, and private study purposes. Any substantial or systematic reproduction, redistribution, reselling, loan, sub-licensing, systematic supply, or distribution in any form to anyone is expressly forbidden.

The publisher does not give any warranty express or implied or make any representation that the contents will be complete or accurate or up to date. The accuracy of any instructions, formulae, and drug doses should be independently verified with primary sources. The publisher shall not be liable for any loss, actions, claims, proceedings, demand, or costs or damages whatsoever or howsoever caused arising directly or indirectly in connection with or arising out of the use of this material.

## Static and Dynamic Observations of Dislocations and Other Defects in Smectic Cano Wedges

I. LELIDIS<sup>ab</sup>, M. KLÉMAN<sup>c</sup> and J.L. MARTIN<sup>a</sup>

<sup>a</sup>*Département de Physique, Institut de Genie Atomique, Ecole Polytechnique Fédérale de Lausanne, CH-1015 Lausanne, Switzerland,* <sup>b</sup>*Permanent address: LPMC Université de Picardie, 80039 Amiens France* and <sup>c</sup>*Laboratoire de Minéralogie-Cristallographie (CNRS-UMR 7590, Universités de Paris VI et Paris VII), 4 place Jussieu, 75252 Paris Cedex 05, France*

We study the role of defects in the flow properties of a thermotropic smectic (in Cano wedge geometry) by in situ deformation experiments in an optical polarizing microscope. The motion of the edge dislocation array is studied for imposed strain rates and their climb velocity is measured. At a stress close to 3000 dyn/cm<sup>2</sup> a jerky climb of edges is observed implying the existence of screw dislocations which hinder the free motion of the former. At a stress close to 5000 dyn/cm<sup>2</sup> a viscous motion of edges is evidenced for which we confirm the validity of the Orowan relation, established for solid crystals.

**Keywords:** thermotropic smectics; defect microstructure; Orowan relation

### INTRODUCTION

We report here on the flow properties of smectics in compression tests, in a manner reminiscent of the plastic flow in solid crystals in

connection with their imperfections. We have observed that the flow is indeed attended by the motion of dislocations<sup>[11]</sup>. As was first pointed out by Orowan<sup>[12]</sup> the rate of deformation is proportional to the number of moving dislocations, their average velocity and the displacement which is carried by each one. In order to verify this law in the case of smectic liquid crystals we observe climbing of edge dislocation directly by optical microscopy and we measure all the quantities related with the imposed deformation rate. This climb motion of edge dislocations could interplay with screw dislocations<sup>[13]</sup> present in the smectic sample, giving rise to deviations from the expected behavior. Therefore we also have to characterize the sample microstructure: screw and edge dislocations respective densities and mutual interactions.

## EXPERIMENTAL PART

The experimental set-up we use is made of a polarized-light optical microscope, an oven (Instec mK) mounted on the stage of the microscope, and a constant strain-rate deformation micro-device containing the sample. Dynamic observations can be carried out during compression tests<sup>[11]</sup>. The normal strain component varies in the range  $\sim 10^{-5}$ - $10^{-3}$ . The liquid crystal compound used is a fluorinated octyloxyphenyl octyloxybenzoate (BDH173, from Merck) with a monotropic SmA-SmC phase transition at 55°C when cooling from the SmA.

A typical sample is composed by two float glass plates in a wedge geometry (fig. 1), treated with a polysilane to ensure homeotropic anchoring. The dihedral angle  $\alpha$  is chosen in the range  $\sim 10^{-4}$ - $10^{-3}$  rad.

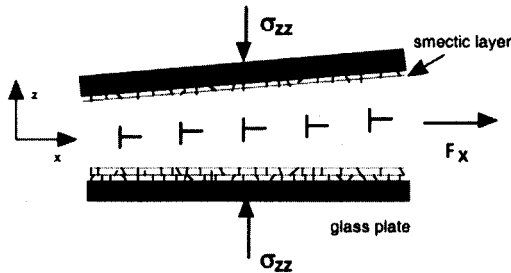


FIGURE 1 Schematic cross section of a wedge-shaped sample, containing a tilt subboundary of edge dislocations.

The wedge geometry gives rise to an edge dislocation tilt subboundary in the SmA phase. Because of the image forces at the glass plates, the tilt subboundary is positioned in the bisector plane of the dihedron. These dislocations become visible (fig. 2) at the vicinity of the SmA-SmC transition<sup>[4]</sup> because the latter starts locally in the stress field of the defects<sup>[5]</sup>. The array period  $\Lambda$  is related to  $\theta$  by:  $\Lambda = b/\theta$ , where  $b = n\alpha$  is the Burgers vector, and  $\alpha$  is the smectic layer thickness ( $\sim 3\text{nm}$ ). Under an applied stress along the layers normal:  $\sigma_{zz} = B \frac{\partial u}{\partial z}$ , where  $B$  is the static compressibility, the edge dislocations should experience a Peach-Koehler force parallel to the layers<sup>[6-8]</sup>:

$$F_x = \pm b \sigma_z,$$

where  $\pm$  is the sign of the dislocation. Under the action of this force the array of edge dislocations should climb to relax the stress. Glide motion of the edge dislocations should be also present. For typical strains, the thickness variation is  $\sim 100$  nm while the climb displacement is  $\sim 10^5$  nm and so the glide motion can be disregarded in a first approximation<sup>[9]</sup>. Furthermore the glide mobility is probably much smaller than the climb mobility, since it requires permeation<sup>[9]</sup>.

## RESULTS ABOUT THE MICROSTRUCTURE

static observations: Figure 2 shows a typical aspect of the microstructure. It consists of the edge dislocations array which are pinned at a forest of screw dislocations: straight dislocation lines anchored on both boundary glass plates and perpendicular to the layers. The above results are further confirmed from cryofractured samples observed by confocal microscopy<sup>[10]</sup>. The origin of the screw dislocations are the hill-shaped surface irregularities on the glass plates, revealed by atomic force microscopy<sup>[10]</sup>. Depending on the glass plates relief and the conditions of the polysilane deposition, the screw density  $\rho_s$ , deduced from the pinning points density on the edges, varies in the range  $\sim 10^5$  to  $10^8$  /cm<sup>2</sup>. These values compare well with the screw dislocation density in lyotropic lamellar phases<sup>[11]</sup>  $\sim 10^7$  /cm<sup>2</sup>. Contrast studies of the polarized and confocal microscopy images are underway to determine the Burgers vector signs and magnitudes<sup>[10]</sup>.

dynamic observations: During their motion, the edge dislocations are slowed down when crossing the forest of screw dislocations to which they are temporarily pinned, in a manner which depends on the sign of their respective Burgers vectors. We observe two edge dislocation mobility regimes depending on the applied stress:

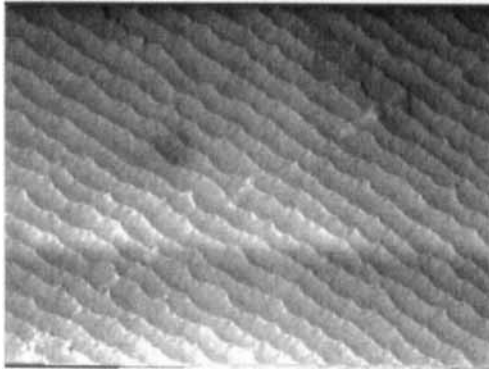


FIGURE 2. Array of edge dislocation ( $n=1$ ) in a wedge-shaped sample near the SmA to SmC transition, viewed between crossed polarizers ( $P \perp A$ ). The edge dislocations are strongly pinned on end on screw dislocations. Cusps visible along the edges result from such an interaction ( $\overline{10} \mu\text{m}$ ).

- a) *jerky climb motion* (fig. 3) for stresses  $\sigma$  lower than a critical value  $\sigma_c$ . Edges are temporarily pinned on screws and their velocity is related to the waiting times at the intersection. The intersection

stress for edges to intersect the screws is estimated from the curvature  $1/R$  of the edge dislocations when they begin to climb<sup>[8]</sup> (the smaller values of  $R$  are considered here) :

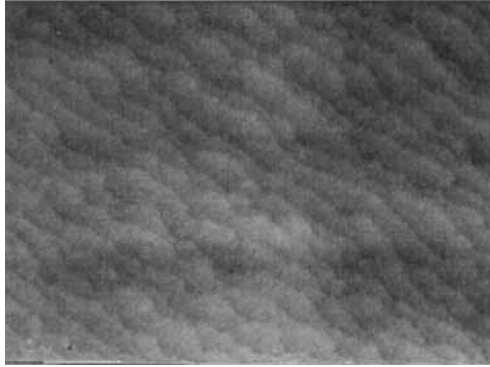


FIGURE 3. Snap-shot of jerky climb motion of edge dislocations ( $\sigma < \sigma_c$ ) temporarily pinned at screw dislocations ( $P \perp A$ ,  $\overline{10} \mu\text{m}$ ).

$$\sigma_{\text{int}} = \frac{Bb}{R} \sim 3000 \text{ dyn/cm}^2,$$

for  $B \sim 10^7 \text{ erg/cm}^3$  and  $n = 1$ .

b) *viscous climb motion* of edge dislocations at stresses higher than  $\sigma_c$  (fig. 4). The climb velocity is controlled by an effective viscosity of the medium. Each edge dislocation moves as a rigid segment.

In a smectic sample under strain, screw dislocations are affected and the strain can give rise to an helical instability<sup>[12, 13]</sup> which will be treated in another publication<sup>[10]</sup>.





FIGURE 4. Snap-shot (PLA) of an edge dislocation array while climbing under stress in the viscous regime ( $\sigma > \sigma_c$ ,  $10\mu\text{m}$ ).

## DISCUSSION

By imposing a controlled velocity  $\dot{\epsilon} = \Delta\epsilon_{zz} / \Delta t$  to one of the glass plates with respect to the other, we are able to check the validity of the Orowan equation :

$$\dot{\epsilon} = \rho_m b v$$

where  $\rho_m$  is the density of mobile dislocations, and  $v$  their climb velocity. Experimentally, we observe that under compression the edge dislocations move towards the thicker part of the sample. The climb

takes place in the plane of the subgrain boundary and all dislocations move parallel to one another (viscous regime).

Figure 5 shows the measured climb velocity as a function of the deformation rate. This graph shows a number of interesting features:

Threshold deformation rate: climb is observed above a threshold deformation rate  $\dot{\epsilon}_c = 0.4 \times 10^{-4} \text{ sec}^{-1}$ . The threshold should correspond to the critical stress for viscous edge dislocations climb motion. Assuming that the response of the material is quasi-elastic for stresses lower than the corresponding critical stress  $\sigma_c$  and using the value of  $B \sim 10^7 \text{ erg/cm}^3$  one calculates  $\sigma_c \sim 5000 \text{ dyn/cm}^2$ , which is an upper value of  $\sigma_c$ .

Orowan relation: for stresses higher than  $\sigma_c$ , a linear variation of the dislocation velocity with the deformation rate is observed. The slope:  $0.15 \text{ cm}^{-1}$  obtained by least square fitting is in good agreement with the expected value of  $\rho_m b = 0.17 \text{ cm}^{-1}$ , where  $\rho_m$  is measured from dislocation distances along the subboundary.

## CONCLUSION

In a smectic liquid crystal, we have evidenced a forest of screw dislocations, the density of which is related to the substrate roughness. As the stress is increased above a value  $\sigma_m \sim 3000 \text{ dyn/cm}^2$ , climbing of edges is observed through the forest of screws, resulting in a jerky motion. Above a critical stress lower than  $5000 \text{ dyn/cm}^2$  a viscous climb

motion of the edge dislocations is observed, for which the Orowan relation has been verified.

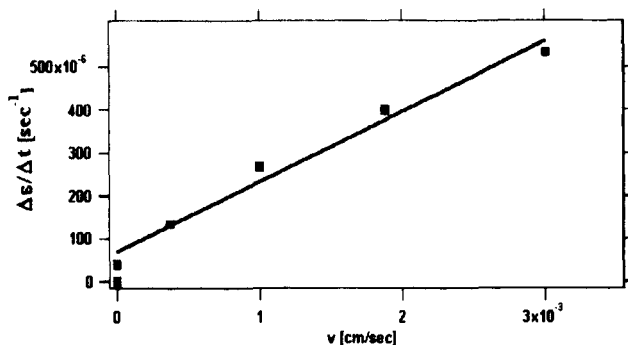


FIGURE 5. Deformation rate versus climb velocity of edge dislocations. The solid line is a least square fitting of the experimental points (solid squares).

Presently, we are carrying a detailed quantitative study of the above phenomena and the multiplication of other defects than dislocations.

### Acknowledgments

We acknowledge the financial support of the *Fonds National Suisse de la Recherche Scientifique*.

### References

- [1] I. Lelidis, M. Kléman and J.L. Martin, accepted in *Mol. Cryst. Liq. Cryst.*, **330**, 457 (1999).
- [2] E. Orowan, *Proc. Phys. Soc.*, **52**, 8 (1940).

- [3] J. P. Hirth and J. Lothe, *Theory of dislocations* (Wiley & Sons, 1982).
- [4] R.B. Meyer, B. Stebler and S.T. Lagerwall, *Phys. Rev. Lett.*, **41**, 1393 (1978).
- [5] R. Ribota, R.B. Meyer and G. Durand, *J. Phys. Lett.*, **35**, L-161 (1974).
- [6] M. Kléman, *J. de Phys.*, **35**, 595 (1974).
- [7] P.S. Pershan, *J. Appl. Phys.*, **45**, 1590 (1974).
- [8] P.S. Pershan, and J. Prost, *J. Appl. Phys.*, **46**, 2343 (1975).
- [9] M. Kléman and C.E. Williams, *J. de Phys. Lett.*, **35**, L-49 (1974).
- [10] I. Lelidis, M. Kléman and J.L. Martin, to be submitted.
- [11] W. K. Chan and W. W. Webb, *J. Phys.*, **42**, 1007 (1981).
- [12] L. Bourdon, M. Kléman, L. Lejcek and D. Taupin, *J. Phys.*, **42**, 261 (1981).
- [13] P. Oswald and M. Kleman, *J. Phys. Lett.*, **45**, L-319 (1984).